Liquid-like behaviour of gold nanowire bridges

Jay P. Naik, , David Cheneler, , James Bowen, and , and Philip D. Prewett

Articles you may be interested in

The mechanism of plasma plume termination for pulse-excited plasmas in a quartz tube
Applied Physics Letters **111**, 074104 (2017); 10.1063/1.4985332

Improving the performance of aeroelastic energy harvesters by an interference cylinder
Applied Physics Letters **111**, 073904 (2017); 10.1063/1.4999765

A silicon nanowire heater and thermometer
Applied Physics Letters **111**, 043504 (2017); 10.1063/1.4985632

Terahertz spectroscopy of an electron-hole bilayer system in AlN/GaN/AlN quantum wells
Applied Physics Letters **111**, 073102 (2017); 10.1063/1.4996925

Self-catalyzed core-shell GaAs/GaNAs nanowires grown on patterned Si (111) by gas-source molecular beam epitaxy
Applied Physics Letters **111**, 072106 (2017); 10.1063/1.4990821

Uniform lifetime prolongation of a high density plasma channel left in the wake of femtosecond filament
Applied Physics Letters **111**, 074102 (2017); 10.1063/1.4994825
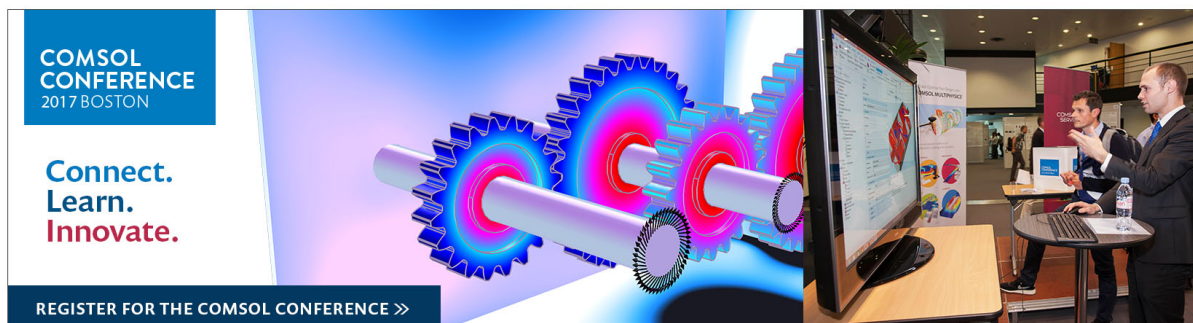
Liquid-like behaviour of gold nanowire bridges

Jay P. Naik,[1] David Cheneler,[2] James Bowen,[3] and Philip D. Prewett[1]

[1]*School of Mechanical Engineering, University of Birmingham, Edgbaston, Birmingham B15 2TT, United Kingdom*
[2]*Department of Engineering, Lancaster University, Lancaster LA1 4YW, United Kingdom*
[3]*School of Engineering and Innovation, The Open University, Milton Keynes MK7 6AA, United Kingdom*

A combination of Focused Ion Beam and Reactive Ion Etch was used to fabricate free standing gold nanowire bridges with radii of 30 nm and below. These were subjected to point loading to failure at their mid-points using an atomic force microscope, providing strength and deformation data. The results demonstrate a dimensionally dependent transition from conventional solid metallic properties to liquid-like behaviour including the unexpected reformation of a fractured bridge. The work reveals mechanical and materials properties of nanowires which could have significant impact on nanofabrication processes and nanotechnology devices such as Nano Electro Mechanical Systems. *Published by AIP Publishing.* [http://dx.doi.org/10.1063/1.4989612]

Focused Ion Beam (FIB) etching has been used by Li *et al.* to fabricate suspended nanowire bridges (NWBs) from Au and Al thin films.[1] A particular feature of their work is the observation that the cross sections of their NWBs relax from trapezoidal to an approximately circular form, which is ascribed to surface energy minimisation, as occurs in liquids. Li *et al.* found further evidence of liquid behaviour in the form of Rayleigh-Plateau instabilities, confirming the earlier results in supported Au nanowires obtained by Naik *et al.*,[2] who observed liquid behaviour with hydrodynamic instabilities for nanowires with radii below a critical radius of approximately 25 nm. These liquid-like instabilities and the critical radius of the nanowires below which bulk material properties no longer apply in a simple form have not been widely studied, due in part to the difficulty of fabricating nanowires below 25 nm in radius. Our previous work[3] explores how a nanowire may undergo a transition in behaviour from solid-like to liquid-like behaviour by treating it as a cylinder. The surface stress is given by

$$\sigma_S = \frac{\gamma}{r_0}, \qquad (1)$$

where γ is the surface tension and r_0 is the radius of the unperturbed wire. If the surface stress is greater than the yield stress, σ_Y, the wire will undergo plastic flow. In addition, liquid-like perturbations of wavelength λ may grow, provided this wavelength is greater than the circumference of the wire, i.e., $\lambda > 2\pi r_0$. The wire may then disintegrate as in the case of the Rayleigh instability of a column of liquid.[3,4] This model suggests that the intermolecular forces between atoms, which are manifested in liquid free surfaces as surface tension, allow a transition from crystalline solid behaviour to liquid-like behaviour below a critical radius[3,5]

$$r_c = \frac{\gamma}{\sigma_Y}. \qquad (2)$$

Assuming $\gamma = 1.145 \, \text{N/m}$[6] and $\sigma_Y = 205 \, \text{MPa}$,[7] $r_c = 6 \, \text{nm}$ for Au nanowires, giving a very approximate value of NWB radius below which a transition from solid-like to liquid-like behaviour might be expected to occur. In the following, we

present experimental results using Au NWBs manufactured using FIB. The NWBs demonstrate solid-like or liquid-like behaviour, depending on their radii. The NWBs are unsupported Au beams of circular cross section, fixed at both ends, which are subjected to an increasing normal load at their mid-points, up to fracture, applied using an Atomic Force Microscope (AFM) cantilever. The NWBs are imaged using scanning electron microscopy (SEM) and AFM (i) before loading and (ii) after the AFM load has been removed.

Au films with thicknesses in the range of 50–100 nm were deposited onto single crystal p-type Si (100) (IDB Technologies, UK) using thermal evaporation (Auto 306, Edwards, UK). FIB etching was performed using a Dual Beam Helios 600 FIB system (FEI, Germany); this instrument also has an SEM for *in situ* inspection. Multiple nanowires, all of nominal length 500 nm, were created with "radii" in the range of 8–30 nm by milling pairs of adjacent trenches through the Au film and into the underlying Si. This produced an intermediate test structure in the form of a flat Au nanowire supported on a Si ridge. The FIB milling process was performed using a Ga^+ beam of energy 30 keV at an estimated beam diameter in the range 10–15 nm and an ion beam current of 20 pA. The milling strategy was to perform two identical rectangular raster scans, sequentially, to form gold on silicon supported a nanowire with length parallel to the longer sides of the scan boxes. The resulting nanowire will receive a small collateral dose of Ga^+ ions due to the beam tails,[8] but this process is different from that of Li *et al.*,[1] who deliberately subjected their gold nanostructures to a broad area, bulk irradiation, with a defined dose of Ga^+ ions in order to observe its effect on surface morphology, including shrinking of features. The Si support was then removed using an undercut reactive ion etch (RIE) process in an STS100 etcher (SPTS Technologies) using etch gas flow rates of 20 sccm of SF_6, 8 sccm of O_2, and 8 sccm of Ar at a pressure of 5 mTorr to produce the suspended Au NWBs. The estimated etch rate was 250 nm/min at an RF coil power of 600 W. These conditions are consistent with an isotropic etch process. Upon removal of the Au/Si interface, the NWB invariably relaxes to a flattened roughly

cylindrical shape, consistent with the results of Li *et al.*[1] This mechanism is due to the removal of forces of adhesion from the Au film as the Si ridge is removed and is evidence that the gold nanobridge becomes suspended; the tendency to minimum free surface energy then produces a roughly cylindrical shape for all the nanowire widths studied. The Au wire nanobridges were deemed to be suspended due to the nature of the isotropic etch in which the undercut of the Si ridge is comparable to the depth of etch for such small geometries. This was further confirmed through mechanical loading using the atomic force microscope which showed deflection of the bridge at load values below those expected for a silicon structure, showing that the latter had been removed.

The mechanical properties of the NWBs were investigated using a NanoWizard II AFM (JPK Instruments, UK), operating a PPP-NCL Si cantilever, presenting a pyramidal tip (Windsor Scientific, UK), whose radius of curvature was approximately 10 nm. The cantilever spring constant was measured as 36.1 N/m using the method described by Bowen *et al.*[9] After first imaging the unloaded NWB using intermittent contact mode AFM, a normal load was applied to the NWB mid-point, with a low positional uncertainty of ∼1 nm along both beam axes; load-displacement data were recorded at a rate of 10 kHz. The AFM load was increased approximately linearly until a fracture-like event was observed in the load-displacement data.

Figure 1 shows SEM images of a 30 nm radius NWB which fractured under mid-point loading. The maximum load applied before fracture was approximately 500 nN; the load-displacement data are shown in Fig. 2(a). The fracture of the NWB results in two Au cantilever beams (AuCBs). The tilted approach and retraction paths of the AFM tip caused frictional contact between the tip and the newly formed, post-fracture AuCBs. This resulted in the right hand AuCB in Fig. 1(b) being pushed downwards as the approach path of the AFM tip extended beyond the point of fracture. The left hand AuCB may then be displaced during withdrawal of the AFM tip.

The stages involved during mid-point loading of NWBs are marked on the AFM load-displacement data shown in Figs. 2(a) and 2(b), which refer to (a) a 30 nm radius NWB and (b) an 8 nm radius NWB. The load-displacement data in Fig. 2 can be interpreted as follows:

(i) The AFM tip makes contact with the NWB. (ii) Initial stages of AFM loading. (iii) Load increases linearly.

(iv) NWB fracture into two cantilevers. (v) AFM tip continues travelling momentarily, whilst in contact with one or both of the cantilevers.

Figure 1 shows NWBs with different radii, imaged using SEM after their fracture under mid-point AFM loading. Figure 1(a) shows a 30 nm radius NWB which appears to have failed in a solid-like fashion, leaving two flat-ended cantilevers. (The load was applied closer to one of the fixed ends of the beam rather than in the middle of the bridge.) Figure 1(b) shows a 20 nm radius NWB which, post fracture, has formed two cantilevers with tapered ends; the NWB exhibits non-uniform thinning, with a sub-10 nm radius along some of its length. Figure 1(c) shows a NWB of 8 nm radius which has retracted post-fracture, leaving bulbous ends on the two resulting stub cantilevers. Figure 1(d) shows two NWBs of 8 nm radius, both of which have formed bulbous-ended cantilevers; the uppermost NWB in the image does not appear to have retracted, and forms a continuous bridge. It exhibits a bright region near the mid-point with a kink out of plane. Figure 3 shows three NWBs with radii of 20 nm (top), 15 nm (middle), and 8 nm (bottom), each of which display retraction post-fracture. It should be noted that the amount of retraction depends on the initial bridge radius, with the thinnest NWB exhibiting the greatest degree of retraction. The cantilevers formed from the 8 nm radius NWB also appear to have bulbous ends, in keeping with those observed in Figs. 1(c) and 1(d).

Consideration of the load-displacement data for a NWB enables the Young's modulus of the material to be estimated from the classical formula for a fixed-fixed cylindrical beam subjected to mid-point loading[10]

$$E = \frac{k_w L^3}{192 I},$$
(3)

where k_w is the spring constant of the NWB, and can be calculated from the AFM load-displacement data. The compound spring constant K of the system of AFM and experimental gold NWB is given by the slope of the loading portion of the AFM load-displacement data, combining the spring constants of both the NWB (k_w) and the AFM cantilever (k_c)
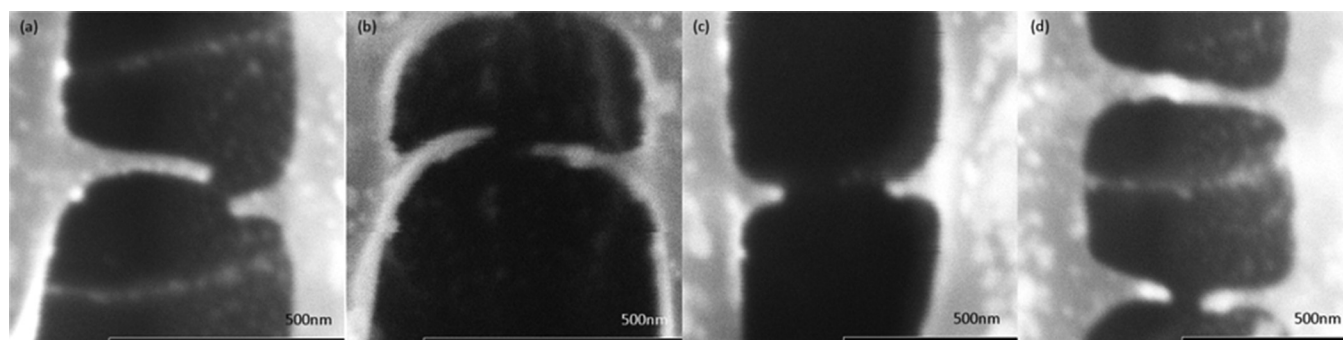

FIG. 1. SEM images of nanowire bridges (NWBs) after fracture. (a) 30 nm radius: flat-ended cantilevers formed; (b) 20 nm radius: tapered cantilevers formed; (c) 8 nm radius: cantilever retraction and bulbous ends formed; and (d) 8 nm radius: bulbous ends on both sets of cantilevers. Retraction is observed only on the lower NWB; the upper NWB has reformed from recoiling cantilevers (see below).
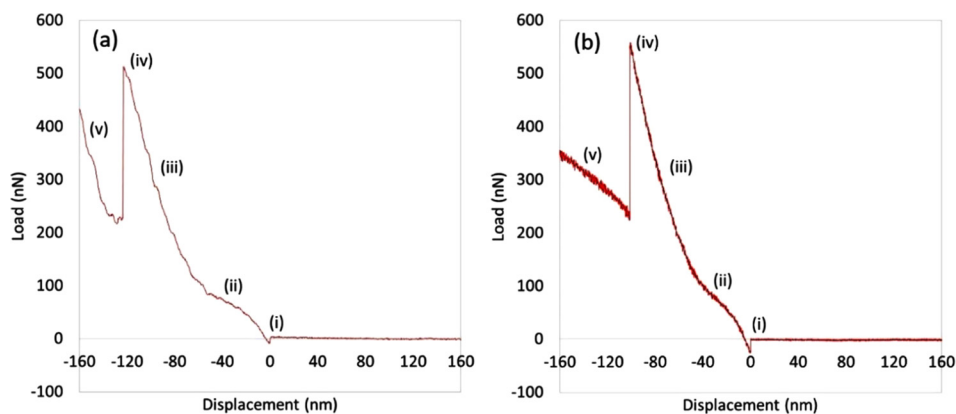
FIG. 2. AFM load-displacement data showing mid-point loading. (a) Nanowire bridge of radius 30 nm: fracture occurs at a mid-point load of 512 nN and (b) nanowire bridge of radius 8 nm: fracture occurs at a mid-point load of 556 nN.

$$K = \frac{k_w k_c}{k_w + k_c}. \tag{4}$$

The second area moment of inertia for a cylindrical beam in Eq. (1), where r is the beam radius, is

$$I = \frac{\pi r^4}{4}. \tag{5}$$

For NWBs of radii 8 nm and 30 nm, the experimental data yield $K_{8\,nm} = 9.6$ N/m and $K_{30\,nm} = 9.3$ N/m, respectively. From Eq. (4), using the AFM cantilever spring constant $k_c = 36.1$ N/m, the spring constants for NWBs of radii 8 nm and 30 nm are $k_{w\,8\,nm} = 13.1$ N/m and $k_{w\,30\,nm} = 12.5$ N/m, respectively. The corresponding elastic moduli are $E_{8\,nm} = 13.4$ GPa and $E_{30\,nm} = 12.8$ GPa. These values are almost an order of magnitude lower than the value for solid Au of approximately 80 GPa, which contradicts the "smaller is stronger" rule.[11] The NWBs therefore do not exhibit the same material properties as bulk Au, having elastic moduli approximately 6× smaller rather than the expected values. This remains unexplained at the present time but may be due in part to Ga$^+$ collateral irradiation during the FIB etching which is discussed further below. (It is known that FIB irradiation creates vacancies and reduces the yield strength in a manner similar to pre-strain treatment.[11,12]) Moreover, a tendency to more liquid behaviour is clearly associated with lower values of elastic modulus.

The energies required to fracture bridges of 30 nm and 8 nm diameter are very close in value at 21.1 fJ and 19.4 fJ, respectively, as found by Marszalek *et al.*[13] After a NWB is fractured, the morphology of the resulting cantilevers depends on the initial radius of the NWB. As the NWB approaches fracture, structural atomic rearrangements occur.[13] According to Marszalek's work, the arrangement of the Au atoms is face centred cubic (fcc) in the bulk material regime. The mid-point loading increases the tensile stress in the bridge so that, prior to fracture and while under stress, slip can occur in the arrangement of the Au crystal planes, changing from fcc to hexagonal close-packed (hcp), which creates stacking faults. At the instant of fracture, the NWB is reduced at its middle to a chain of Au atoms. When a strained Au-Au bond in this chain breaks, the reaction force within the Au atoms in the resultant cantilever may cause a spring-like recoil effect due to the elastic strain energy stored during AFM compressive loading. However, this cannot explain the bulk rearrangement observed after fracture for NWBs of smaller radii; such effects are indicative of liquid-like behaviour. Thus, when a NWB with $r < r_c$ is broken, surface tension significantly influences the morphology of the two cantilevers formed. We conclude that surface tension drives the formation of the curved meniscuses seen at the fixed end of the cantilevers in Figs. 1(c) and 1(d).

The minimum energy surface shape is a spontaneous phenomenon associated with liquids and cannot be explained using a solid crystalline model. However, the critical radius model is an approximation and, not unexpectedly, the onset of liquid-like behaviour does not have a sharp threshold as a function of NWB radius; NWBs with radii slightly greater than r_c display a combination of solid-like and liquid-like behaviour. There is some evidence of this combination of behaviours in a structure of very small radius (8 nm diameter) in the form of the continuous NWB in Fig. 1(d) upper. Our explanation is that this NWB has reformed from the two AuCBs which were created from fracture of the original NWB. These have come into contact by elastic recoil (solid-like behaviour) or through "stiction" with the AFM tip which then drags the fractured parts back into contact where they coalesce—driven by surface tension—to reform the bridge (liquid-like behaviour). The bright kinked region in the SEM image is interpreted as the location in the reformed NWB
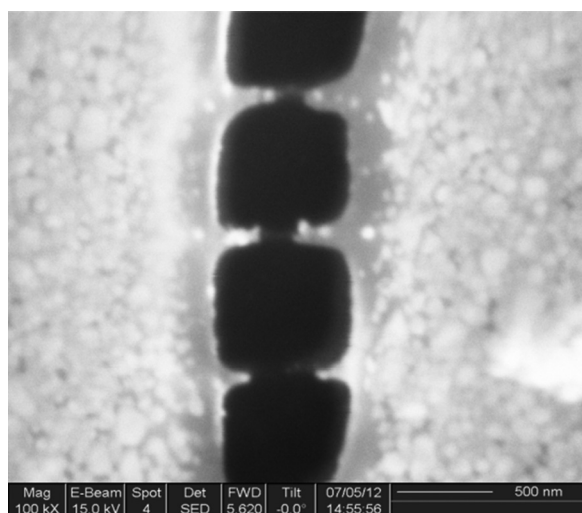

FIG. 3. SEM image of nanowire bridges (NWBs) with radii of 20 nm (top), 15 nm (middle), and 8 nm (bottom); an increasing amount of retraction is observed with decreasing NWB radius.

where the two ends of the cantilevers have come together. Thus, the upper NWB in Fig. 1(d) is an example of combined solid-like and liquid-like behaviour in a very narrow (8 nm wide) bridge.

Differences in the predicted and actual radii at which liquid-like behaviours are observed may be due to the presence of traces of Ga in the Au NWBs, arising from the FIB etch process used to form the nanowire. Implanted Ga ions would modify the surface tension value and disrupt the atomic structure of the Au bulk, which could explain the significantly reduced elastic moduli calculated above. Under the experimental conditions employed in this work, the range of Ga implantation into a surface will be ∼10 nm from the target location, approximated by a sum of Gaussian density distributions.[14,15] Hence, all of the experimental NWBs will contain some implanted gallium atoms.

Focused ion beam and reactive ion etching were used in combination to fabricate Au nanowire bridges with radii ranging from 8 to 30 nm. An atomic force microscope was used to carry out mechanical strain experiments on the suspended nanowire bridges, by subjecting them to mid-point loading until the fracture point was reached. The results show that nanowire bridges with 30 nm radius undergo fracture in a conventional solid-like fashion. In contrast, nanowire bridges with 8 nm radius appear to undergo post-fracture flow retraction of Au atoms, in a mechanism which is clearly liquid-like. Intermediate behaviour is observed for nanowire bridges of 15 nm radius. The results also show that the relative extent of Au retraction, post-fracture, increases with decreasing nanowire bridge radius. The experimental evidence supports the idea that metal nanowires near or below a critical radius show a transition from solid-like to liquid-like behaviour. A remarkable result for a very narrow nanowire bridges of radius 8 nm is the appearance of a reformed bridge where two elastically recoiling cantilevers have come together following fracture of the bridge with liquid flow leading to bridge reformation—a combination of solid and liquid-like behaviour.

[1]C. Li, L. Zho, Y. Mao, W. Wu, and W. Xu, "Focused-ion-beam induced Rayleigh-Plateau instability for diversiform suspended nanostructure fabrication," Sci. Rep. **5**, 8236 (2015).

[2]J. P. Naik, P. D. Prewett, K. Das, and A. K. Raychaudhuri, "Instabilities in focused ion beam patterned Au nanowires," Microelectron. Eng. **88**, 2840 (2011).

[3]J. P. Naik, K. Das, P. D. Prewett, A. K. Raychaudhuri, and Y. Chen, "Liquid-like instabilities in gold nanowires fabricated by focused ion beam lithography," Appl. Phys. Lett. **101**, 163198 (2012).

[4]Lord Rayleigh, "On the instability of jets," Proc. London Math. Soc. **S1–10**, 4 (1878).

[5]S. V. Aradhya, M. Frei, M. S. Hybertsen, and L. Venkataraman, "Van der Waals interaction at metal/organic interfaces at the single molecule level," Nat. Mater. **11**, 872 (2012).

[6]S. M. Kaufmann and T. J. Whalen, "The surface tension of liquid gold, liquid tin and liquid gold-tin binary solutions," Acta Metall. **13**, 797 (1965).

[7]G. W. C. Kaye and T. H. Laby, *Tables of Physical and Chemical Constants* (Longmans, Green and Co., London, 1911).

[8]M. Kolibal, T. Matlocha, T. Vystavel, and T. Sikola, "Low energy focused ion beam milling of silicon and germanium nanostructures," Nanotechnology **22**, 105304 (2011).

[9]J. Bowen, D. Cheneler, D. Walliman, S. G. Arkless, Z. Zhang, M. C. L. Ward, and M. J. Adams, "On the calibration of rectangular atomic force microscope cantilevers modified by particle attachment and lamination," Meas. Sci. Technol. **21**, 115106 (2010).

[10]J. M. Gere and S. P. Timoshenko, *Mechanics of Materials*, 4th ed. (Brooks/Cole, USA, 1997).

[11]Seok - Woo Lee, D. Mordehai, E. Rabkin, and W. D. Nix, "Effects of focused ion beam irradiation and pre-strain on the mechanical properties of FCC Au microparticles on a sapphire substrate," J. Mater. Res. **26**, 221 (2011).

[12]D. Guo, G. Xie, and J. Luo, "Mechanical properties of nanoparticles: Basics and applications," J. Phys. D: Appl. Phys. **47**, 013001 (2013).

[13]P. E. Marszalek, W. J. Greenleaf, H. Li, A. F. Oberhauser, and J. M. Fernandez, "Atomic force microscopy captures quantized plastic deformation in gold nanowires," Proc. Natl. Acad. Sci. U.S.A. **97**, 6282 (2000).

[14]A. Sabouri, C. J. Anthony, P. D. Prewett, J. Bowen, and H. Butt, "Effects of current on early stages of focused ion beam nano-machining," Mater. Res. Express **2**, 055005 (2015).

[15]P. D. Prewett and G. L. R. Mair, *Focused Ion Beams from Liquid Metal Ion Sources* (Research Studies Press, Taunton, 1991).